

Electronic Supplementary material to PCCP manuscript B705046A

“Fabrication of magnetically functionalized lens- and donut-shaped microparticles by a surface formation technique”

by Hartmut A. Wege^{a,b}, Amro K. F. Dyab^a, Orlin D. Velev,^b and Vesselin N. Paunov*^a

^a Surfactant & Colloid Group, Department of Chemistry, University of Hull, Hull, HU6 7RX, UK. Fax: +44(0)1482 466410; Tel: +44(0)1482 465660; E-mail: V.N.Paunov@hull.ac.uk

^b Department of Chemical and Biomolecular Engineering, North Carolina State University, Raleigh, NC 27695-7905, Fax: +1 (919) 515-3465; Tel: +1(919) 513-4311, E-mail: odvelev@unity.ncsu.edu

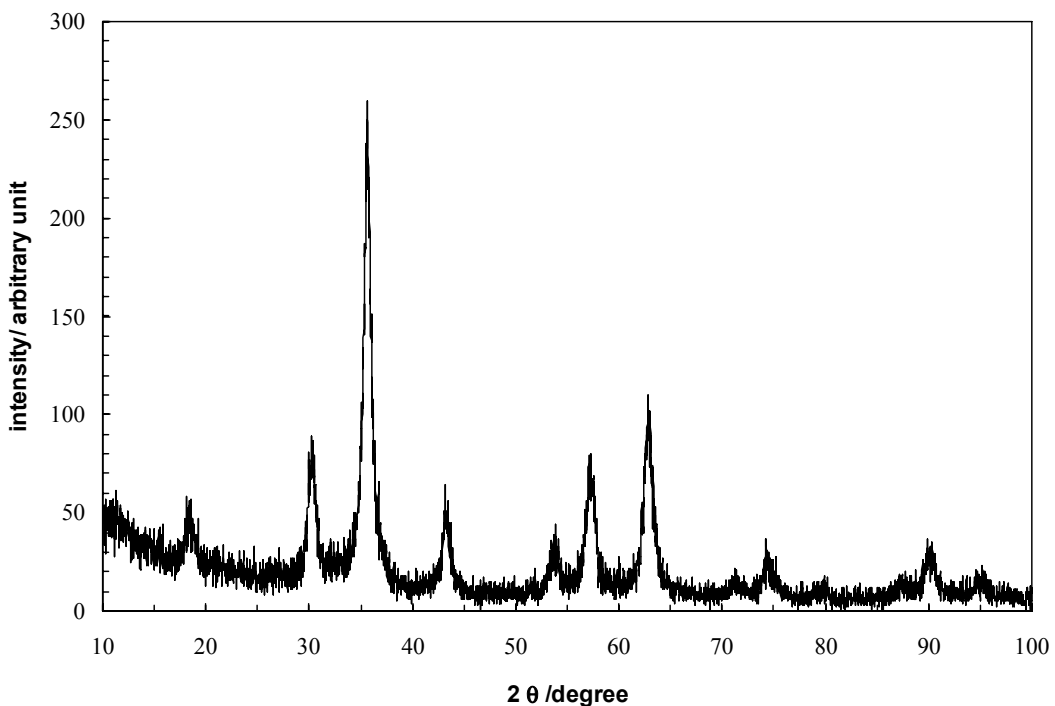


Figure 1. XRD patterns of oleic acid-coated magnetite nanoparticles powder.

Figure 1 shows the X-ray diffraction analysis for the oleic acid-coated magnetic nanoparticles powder. The XRD patterns revealed diffraction peaks which are characteristic of the Fe_3O_4 crystal with a cubic spinel structure. The position and the relative intensity of all diffraction peaks were identical with standard spectra for bulk magnetite, except for the broadening of the peaks. No other phase/impurity was detected. The crystallite size of the magnetic particles was estimated from the XRD patterns using Scherrer formula¹

$$D = \frac{0.9\lambda}{(B_{\text{sample}}^2 - B_{\text{standard}}^2)^{0.5} \cos \theta}$$

where D is the crystallite size in Å, λ is X-ray wavelength (1.54059 nm), 0.9 is constant (K) which depends on the both apparatus and the studied sample ($0.1 < K < 1.3$), B_{sample} and B_{standard} are the full width at half-maximum (FWHM) of the sample peak and standard material respectively and θ is Bragg angle. B and θ are in radiant. The calculated crystallite size was found to be 21.5 nm.

The powder sample was scanned for XRD using the Siemens D5000 X-ray diffractometer. The instrument peak width calibration was obtained using a well-crystallized silicon powder.

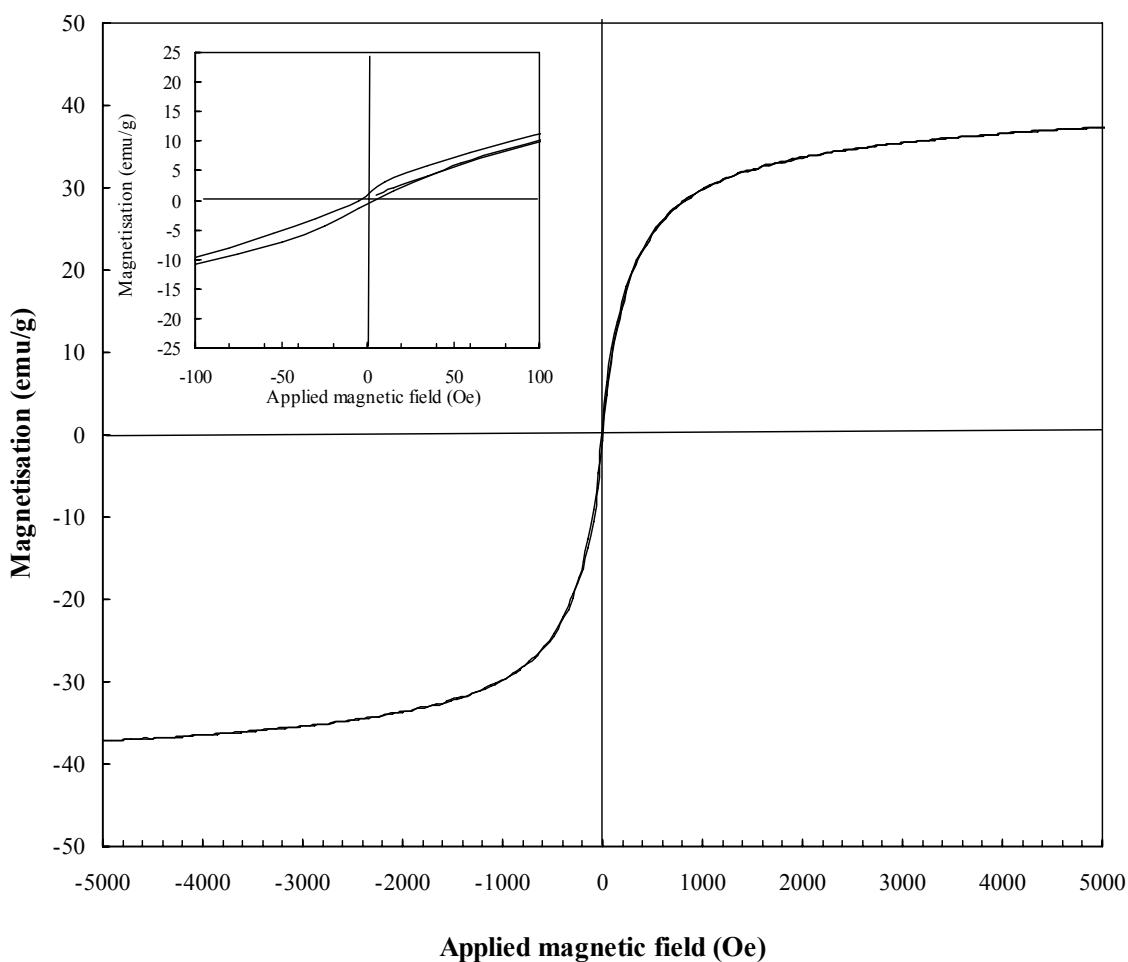


Figure 2. Magnetization curve of oleic acid-coated magnetic nanoparticles at 298 K. The inset shows the hysteresis loop near the zero magnetic field region.

Magnetic characterisations of the particles were measured using the vibrating sample magnetometer (VSM) (Lake Shore 7300, USA) at room temperature (298 K) with an applied field $-10 \leq H \leq +10$ KOe. The magnetization unit was emu/g, after it was normalized by the weight of the sample (fixed for all different samples).

Figure 2 shows the magnetisation curve of oleic acid-coated magnetic nanoparticles at 298 K. The saturation magnetisation (M_s) was found to be 39.35

emu/g, the remanence magnetisation (M_r) was 1.4 emu/g and the coercivity (H_c) was 4.6 Oe. The very low values of remanence and coercivity (as clearly seen in the inset of Figure 2) are consistent with good superparamagnetic behaviour and that the magnetic particles have essentially single domains.² It was estimated that the critical size of magnetite particles (D_p), in which ferromagnetism transfers to superparamagnetism was 25 nm at room temperature based on the theoretical calculation.³ Since the magnetic nanoparticles used in this work have a diameter equal to 21.5 nm which is below D_p (25 nm) and thus ensuring superparamagnetic behaviour. According to Figure 2, we found that the M_s value for oleic acid-coated magnetic nanoparticles is lower than that of bulk magnetite (90 emu/g).⁴ Similar reduction in M_s has been reported for magnetite particles coated with oleic acid⁴ or other materials.⁵ The reason for this reduction is not clear as it may vary with different preparative methods but it was attributed to a possible existence of disordered spins at the surface.⁶ In contrast, other studies^{7,8} showed that oleic acid-coated magnetite nanoparticles exhibited saturation magnetisation, M_s , close to that expected for bulk magnetite in contrast with most reported M_s values. The authors suggested that the oleic acid molecules covalently bonded to the nanoparticles surface yield a strong reduction in the surface spin disorder. It is obvious that different results and interpretation are reported as the preparation methods are completely varied.

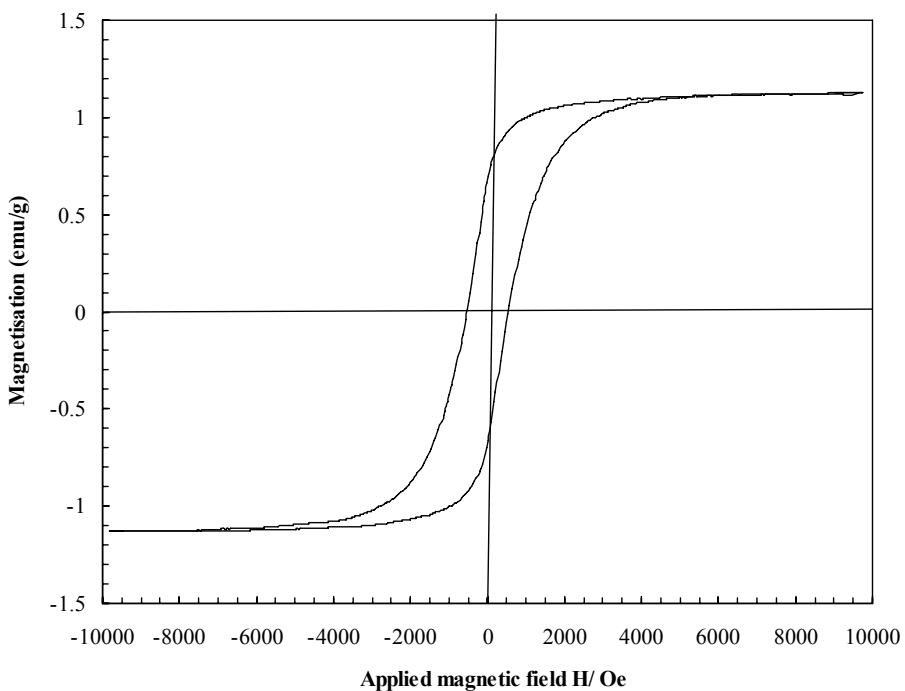


Figure 3. Magnetization curve of magnetite doped (10% w/w) microlenses produced by spreading IPA solution of paraffin/ceresin at $T = 55$ °C in the presence of external magnetic field which is perpendicular to the air-water interface.

Figure 3 shows the magnetisation curve of donut-shaped microparticles doped with (10% w/w) oleic acid-coated magnetic nanoparticles at 298 K. The hysteresis loop, which is a similar to the ferromagnetic behaviour, can be clearly seen. For this sample, the saturation magnetisation (M_s) was found to be 1.1 emu/g, the remanence magnetisation (M_r) was 0.7 emu/g and the coercivity (H_c) was 535 Oe. The high H_c and M_r values signify that the microparticles retained magnetisation at zero applied field which is a typical ferromagnetic behaviour. The remanence ratio M_r/M_s is a test for differentiating between SD (single-domain) and non-SD particles behaviour. According to the Stoner and Wohlfarth model⁹, a remanence ratio of 0.5 results only if a random distribution of non-interacting uniaxial particles is present, while a remanence ratio of less than 0.1 is typically observed in the multi-domain case. The remanence ratio (M_r/M_s) for these microparticles was found to be 0.6 which is close to the value of 0.5 for a system of noninteracting single domain particles with uniaxial anisotropy. This means that the thermal agitation energy cannot overcome the anisotropy energy barrier for a single particle.⁴ This remarkable difference in magnetisation properties of the magnetic donut-shaped microparticles and the oleic acid-coated nanoparticles might be attributed to several reasons. It might be due to the increased anisotropy of the core magnetic particles induced by the freezing the alignment of these particles during the application of perpendicular external magnetic field while preparing the microparticles on the surface of the surfactant solution. Similar trend has been confirmed with our undergoing work with polymer anisotropic magnetic particles.

Best donuts microparticles images showing some magnetic contents:

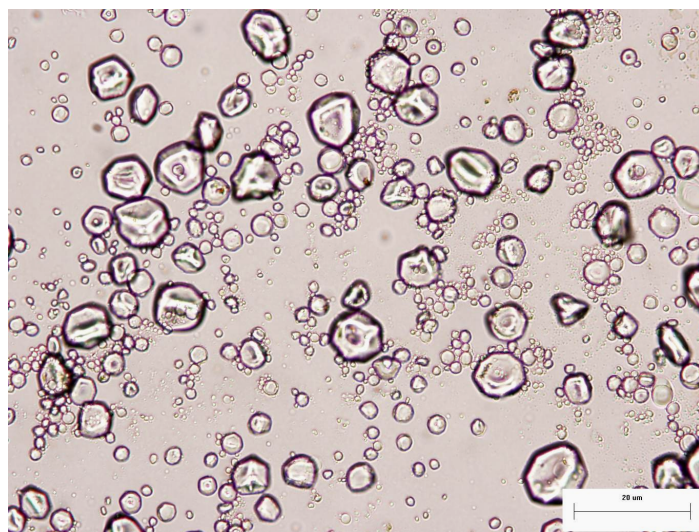


Figure 4. Optical micrograph of doped (10% w/w) microlenses of various morphologies produced by spreading IPA solution of paraffin/ceresin at $T = 55\text{ }^{\circ}\text{C}$ in the presence of external magnetic field which is perpendicular to the air-water interface. The aqueous subphase is 10 mM SDBS.

Microparticles size distribution was measured using Malvern Mastersizer 2000 at room temperature. The mean diameter was found to be $20.1\text{ }\mu\text{m}$ which is consistent with the estimated average particles diameter ($17.9\text{ }\mu\text{m}$) obtained from different microscopic images.

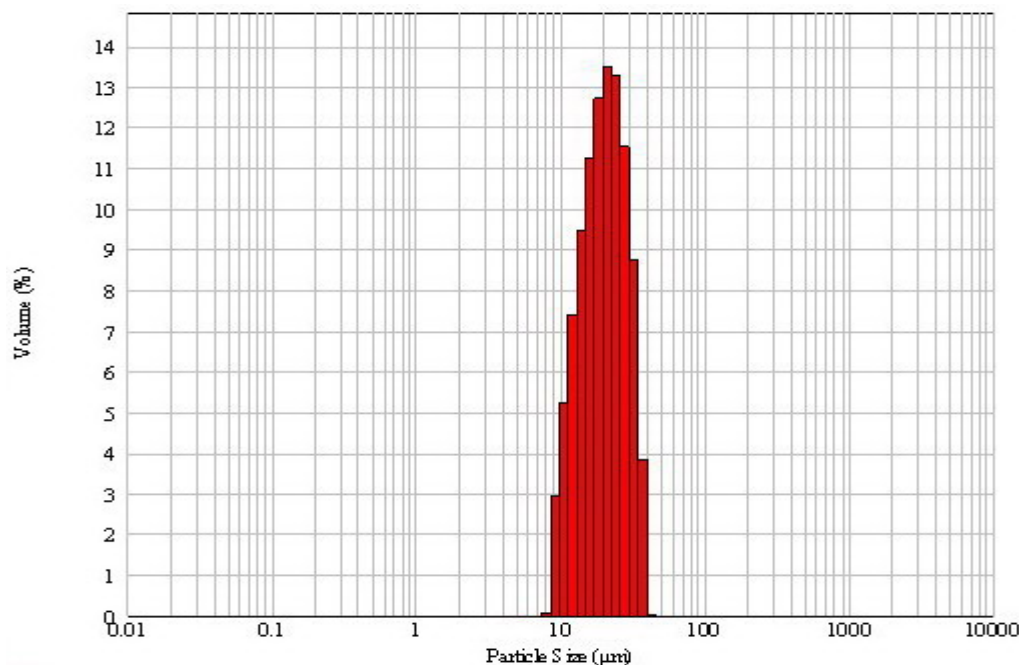


Figure 5. Size distribution of magnetic microlenses shown in Figure 4 measured using laser diffraction method showing the mean diameter of 20 μm .

References:

1. L.E. Smart and E.A. Morre, *Solid State Chemistry: an Introduction*, Taylor & Francis, P.89 (2005).
2. Z. Huang, F. Tang and L. Zhang, *Thin Solid Films*, **471**, 105 (2005).
3. J. Lee, T. Isobe and M. Senna, *J. Colloid Interface Sci.*, **177**, 490 (1996).
4. X.Liu, M.D. Kaminski, Y. Guan and H. Chen, *J. Magn. Magn. Mater.*, **306**, 248 (2006).
5. M. Yamaura, R.L. Camilo, L.C. Sampaio and M.A. Macedo, *J. Magn. Magn. Mater.*, **279**, 210 (2004).
6. R.H. Kodama, *J. Magn. Magn. Mater.*, **200**, 359 (1999).
7. P. Guardia, B. Batlle-Brugal, A.G. Roca, O. Iglesias, M.P. Morales, C.J. Serna, A. Labarta and X. Batlle, *J. Magn. Magn. Mater.*, (2007), doi:10.1016/j.jmmm.2007.03.085
8. A.G. Roca, M.P. Morales, K.O'Grady and C.J. Serna, *Nanotechnology*, **17**, 2783 (2006).
9. E.C. Stoner and E.P. Wohlfarth, *Philos. Trans. R. Soc. Lond. Scr. A*, **240**, 599 (1948).